



UWS Academic Portal

Correlation of Ca/Si and micromechanical properties in leached grey and white cement pastes

Howind, Torsten; Hughes, John; Zhu, Wenzhong

Published: 01/01/2012

Document Version

Publisher's PDF, also known as Version of record

[Link to publication on the UWS Academic Portal](#)

Citation for published version (APA):

Howind, T., Hughes, J., & Zhu, W. (2012). Correlation of Ca/Si and micromechanical properties in leached grey and white cement pastes. Paper presented at 34th International Conference on Cement Microscopy, Halle, Germany.

General rights

Copyright and moral rights for the publications made accessible in the UWS Academic Portal are retained by the authors and/or other copyright owners and it is a condition of accessing publications that users recognise and abide by the legal requirements associated with these rights.

Take down policy

If you believe that this document breaches copyright please contact pure@uws.ac.uk providing details, and we will remove access to the work immediately and investigate your claim.

CORRELATION OF CA/SI AND MICROMECHANICAL PROPERTIES IN LEACHED GREY AND WHITE CEMENT PASTES

Howind, T., *Hughes, J. J. and Zhu, W.

School of Engineering, University of the West of Scotland, Paisley Campus, PA1 2BE

*corresponding author, john.hughes@uws.ac.uk +44 141 848 3268

ABSTRACT

Grey and white Portland cement pastes were prepared and hydrated for 28 days and then partially calcium leached in a 6M ammonium nitrate solution. The samples were then subjected to micromechanical and compositional analysis. Polished surfaces were interrogated using nanoindentation for Young's Modulus and Hardness. Indents and hydration structures were then imaged in a FESEM, and EDS applied for elemental analysis across a traverse from the exterior to interior of the samples to ascertain the degree of change to Ca/Si in non-degraded and degraded portions of samples. A good agreement is seen between Ca/Si and mechanical properties. The microstructure of the degraded parts shows evidence of increased porosity and alteration to unhydrated binder components. Adequate sample preparation was a critical factor for nanoindentation, to ensure high flatness of the sample surface prior to testing. This results also in an improvement in SEM imaging, and phase discrimination.

INTRODUCTION

The *fairly* slow process of calcium leaching can be a matter of concern for cement and concrete durability in cases where the material is permanently in contact with running water, and the affected surface cannot be accessed for maintenance (e.g. concrete pipes, tunnels). The osteoporoses-like process of calcium leaching leads to an increased micro-porosity caused by a progressive dissolution of calcium out of the microstructure of cement paste. It detrimentally affects the load bearing capacity of cement-based materials but also affects their deformation behaviour [1, 2, 3, 4, 5, 6, 7]. The kinetics of the process depend on several parameters; porosity (the natural path for chemical attack), the composition of the paste (each phase degrades at a different rate), and the nature of the aggressive solution (usually soft water). It is generally agreed that the response of each hydration product to calcium leaching is different and depends on the Ca/Si ratio [8]. Portlandite (CH), the hydration product most severely affected by calcium leaching, leaches out quickly (and completely) leaving new pores in its place. Calcium silicate hydrate (C-S-H) dissolves to a precipitate with a lower Ca/Si ratio leading to a progressive homogenisation of the paste. Nevertheless, the loss of calcium leads in all cases to an increasing porosity and a reduced strength [e.g. 2, 3]. This paper presents selected results of a study into the properties of leached cement pastes.

MATERIALS AND METHODS

Materials and sample preparation

For this study two commercially available ordinary Portland cements (CEM I, 52.5N), provided by *Italcementi*, were used. Cement pastes of grey (OPC) and white (WOPC) Portland cement were prepared with a fixed water cement ratio of $w/c = 0.40$. The compositions and physical characteristics of the cements used are given in Table 1.

Table 1: Compositions and physical characteristics of the cements used

	C ₃ S	C ₂ S	C ₃ A	Gypsum	Anhydrite	Density	Blaine
OPC	65.7 %	10.5 %	8.4 %	1.9 %	2.3 %	3.13 g/cm ³	470 m ² /kg
WOPC	87.1 %	6.0 %	1.1 %	4.1 %	1.7 %	3.08 g/cm ³	296 m ² /kg

After 1 day in the mould the specimens (typically 10 x 10 x 60 mm³) were demoulded and then immediately sealed in aluminium foil and stored in lab conditions (20 ± 3°C) for curing. After 28 days the hydration was stopped by rinsing the paste specimens several times with isopropyl alcohol (as C₃H₈O replaces water in the paste). The specimens for investigating the non-degraded pastes were then stored in a desiccator (with silica gel) to remove the remaining free water from the samples. To obtain degraded cement paste samples the accelerated calcium leaching started after 28 days of hydration by immersing the specimens in a 6M ammonium nitrate solution (480 g/l NH₄NO₃). The NH₄NO₃ solution was renewed whenever the pH value reached 9.2. The accelerated calcium leaching was stop after 12 days. The leaching stage was tested with phenolphthalein showing pink colour sample interior . For the subsequent tests and further preparation the partially leached specimens were cut into segments (10 x 10 x 10 mm³) and embedded in epoxy resin disks.

Cement paste as a multiphase composite material consists of many different phases with big differences in stiffness/hardness among them (from 0 GPa for pores to 130 GPa for un-hydrated clinker). Thus it is extremely difficult to achieve a very smooth surface of $R_q \ll 100$ nm required for the low-depth indentation testing carried out at different stages of degradation respectively hydration. To avoid the loss of weak phases and to support especially the low strength microstructure for calcium leached cement paste specimens during the grinding and polishing procedures a vacuum resin impregnation of the different specimens was performed (Fig. 1 and Fig. 2). After impregnation with resin suitable for the different strength level of the materials we started with grinding steps down to 1200 grit using abrasive paper and alcohol-based lubricant to avoid potential rehydration or dissolution of hydration products. For the same reason only oil-based lubricant and diamond suspension sprays were used for the following ‘*long-term - low speed - low contact pressure*’ polishing. This procedure consists of 3 steps of at least 90 minutes each using diamond suspensions of 6, 1 or 0.25 μm particle size.

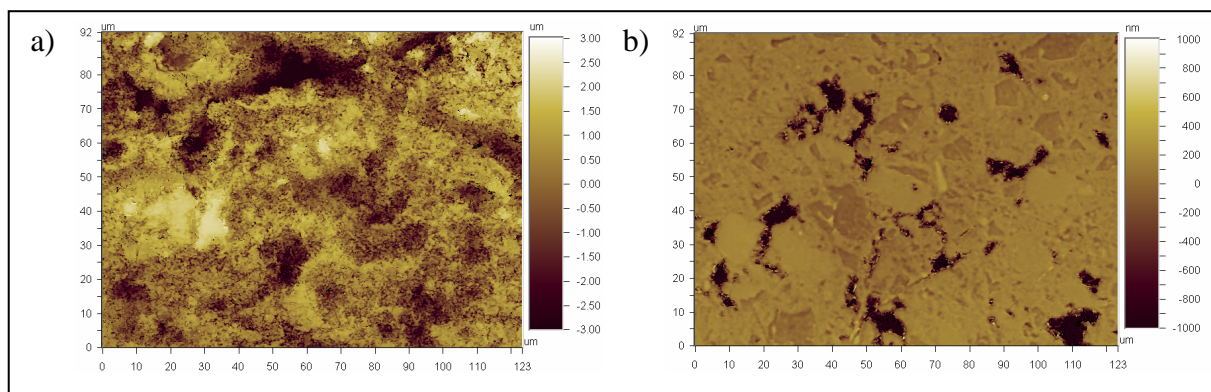


Fig. 1 Preferential polishing and loss of weaker phases of early aged and leached cement paste specimens (White-Light-Interferometer images, 123 x 92 μm²). a) High surface roughness due to preferential polishing without resin impregnation, $R_q = 1.21$ μm; b) Loss of weaker phases due to ‘Pop outs’ in the surface.

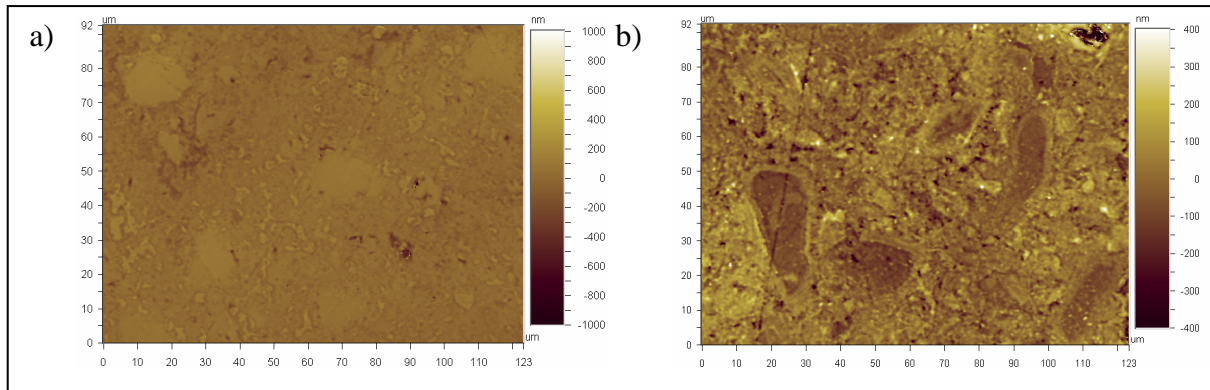


Fig. 2 Low surface roughness of impregnated cement specimens achieved (White Light interferometry, $123 \times 92 \mu\text{m}^2$); a) 28 days hydrated WOPC paste, $R_q = 60 \text{ nm}$; b) Partially calcium leached WOPC paste, $R_q = 80 \text{ nm}$.

Methodology

Nanoindentation is a very versatile technique which allows the determination of mechanical properties such as Young's modulus (E) and hardness (H) on a micro-scale. The methodology and operating principle for the nanoindentation technique have been reviewed and presented in detail elsewhere [e.g. 9, 10, 11, 12, 13]. As a load is applied to an indenter in contact with the surface of a specimen, an indent is produced consisting of elastic and plastic deformation. The recovery of the elastic deformation occurs at the start of unloading. Thus, analysing the initial part of the unloading data allows the determination of the Young's modulus, E , for the indented area. The nanoindentation apparatus used in this study was an Agilent Nano Indenter[®] G200 fitted with a Berkovich indenter tip. A progressive multistep indentation testing with two load-unload cycles were performed at each test point. The unloading data of the second cycle ($h_p \approx 200 \text{ nm}$) were used to determine the E modulus values (Fig. 3).

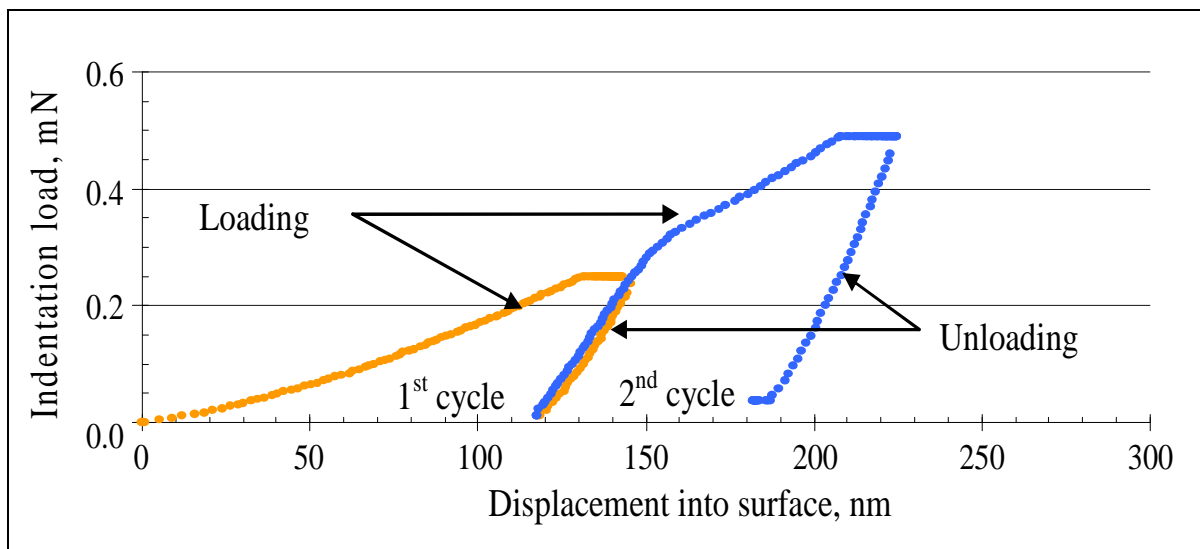


Fig. 3 Typical $P - h$ curve of a two-step nano-indentation test

In order to better observe the gradual change in mechanical performance a test setup consisting of 400 indents (4 rows with $50 \mu\text{m}$ indent spacing) following a traverse of 5 mm length from the exterior to interior of the samples, a distance of 5 mm , was used on the partially leached specimens. To ease the navigation on the sample during the SEM/EDS work the tested area was also marked with an additional row of very large indents ($h = 2000 \text{ nm}$) easy to spot under

a microscope. On top additional large indents were performed to subdivide the test area into smaller blocks of 500 μm length helping to determine distance within the sample (Fig. 4).

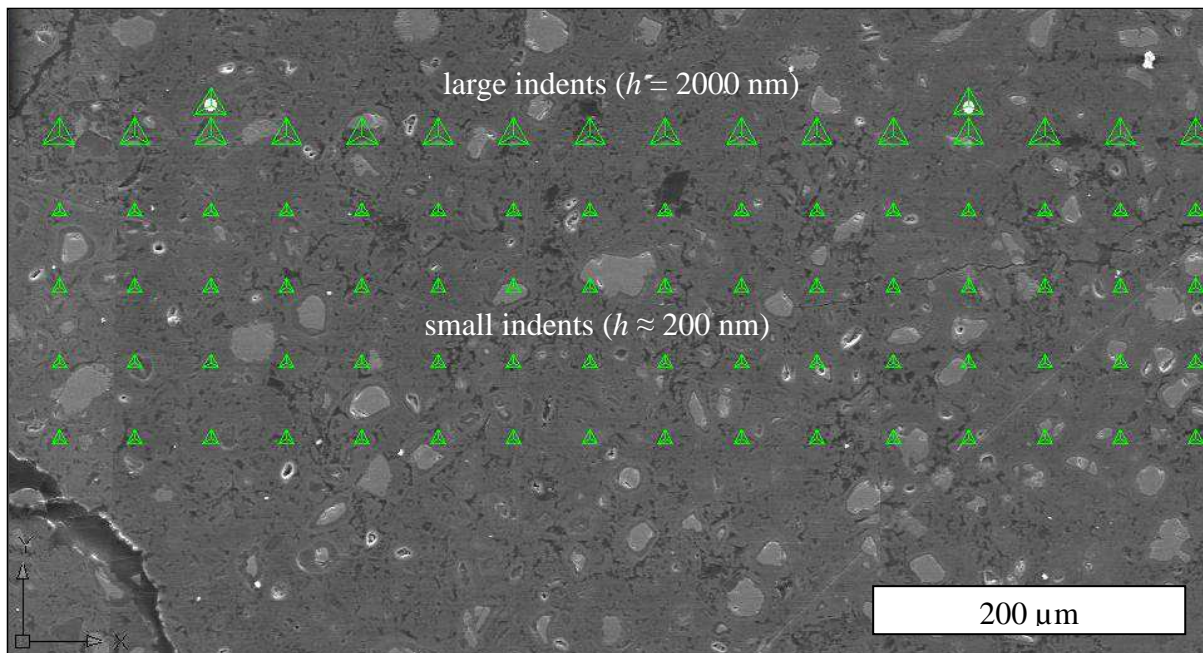


Fig. 4 Nanoindentation test setup, with large visible indents on top serving as guidance for later SEM/EDS analysis and 4 rows of low depth nanoindentation test points of the mechanical properties testing.

After the nanoindentation experiment each tested sample area was studied using a Field-Emission Scanning Electron Microscope (FEG-SEM Hitachi S-4100), using secondary (SE) imaging in conjunction with energy-dispersive spectroscopy analysis (EDS, Oxford Systems INCA) to determine qualitatively and quantitatively the mineral compositions within the tested areas, normally at 15 kV. Samples were carbon coated and cobalt gain calibration was utilised. For both OPC and WOPC EDS analysis was applied to collect a line-scan from the leached exterior to the unleached interior of the samples, parallel and within the tracks of the nanoindentation traverse, from which Ca/Si ratio was calculated from the normalised count intensities for each element.

RESULTS

Our general aim within this study was to improve our knowledge of the link between the structural/compositional changes observable in the SEM and changes in mechanical performance related to hydration and degradation. The improved understanding of such links is very valuable for future work helping to increase mechanical and durability performance of cementitious materials using computer-based simulation. Like all multiphase composite materials cement paste obtains strength from the interaction of its ingredients. The preparation of a partially leached specimen was chosen to investigate the structural changes within one sample with a focus mainly on the Ca/Si ratio alongside the mechanical strength of the hydration products.

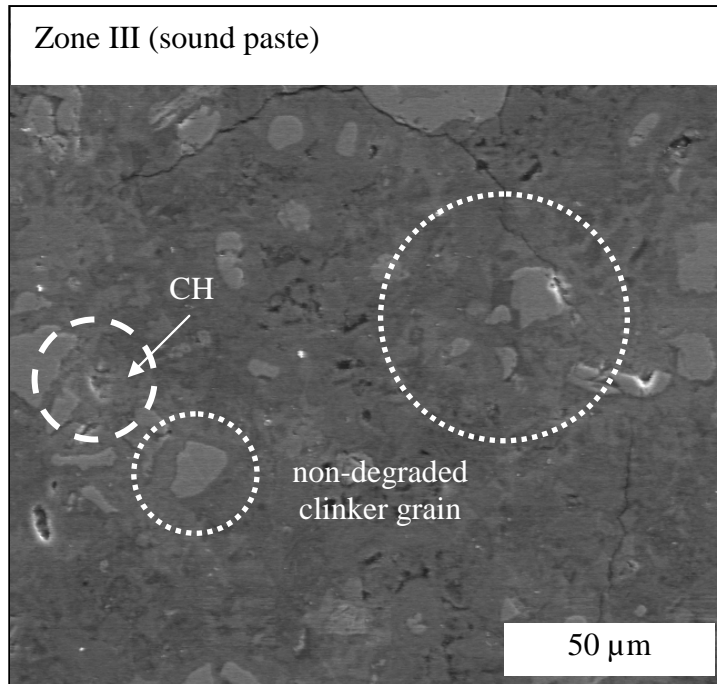


Fig. 5 SEM-SE image of sound cement paste showing the presence of CH and no sign of degradation on the unhydrated clinker grains.

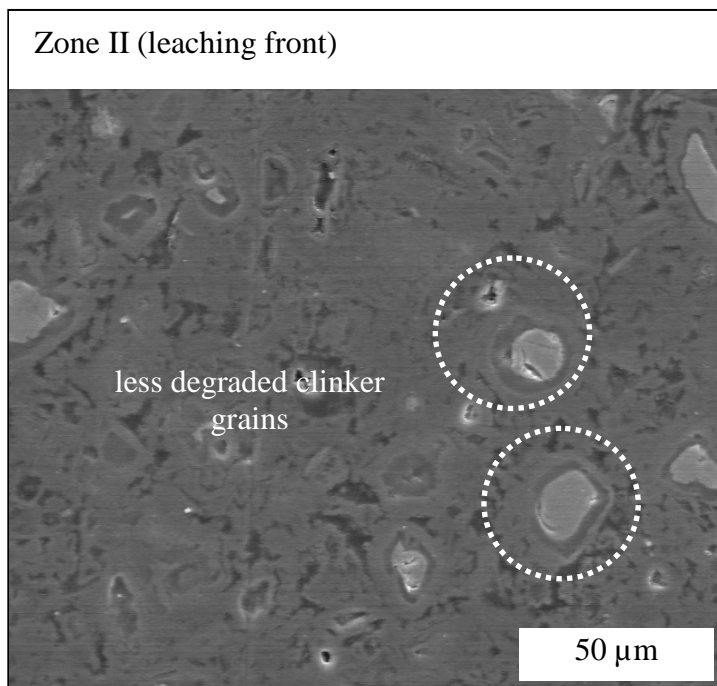


Fig. 6 SEM-SE image No indications for the presence of CH in the paste within the leaching front, beginning degradation of the cement clinker grains.

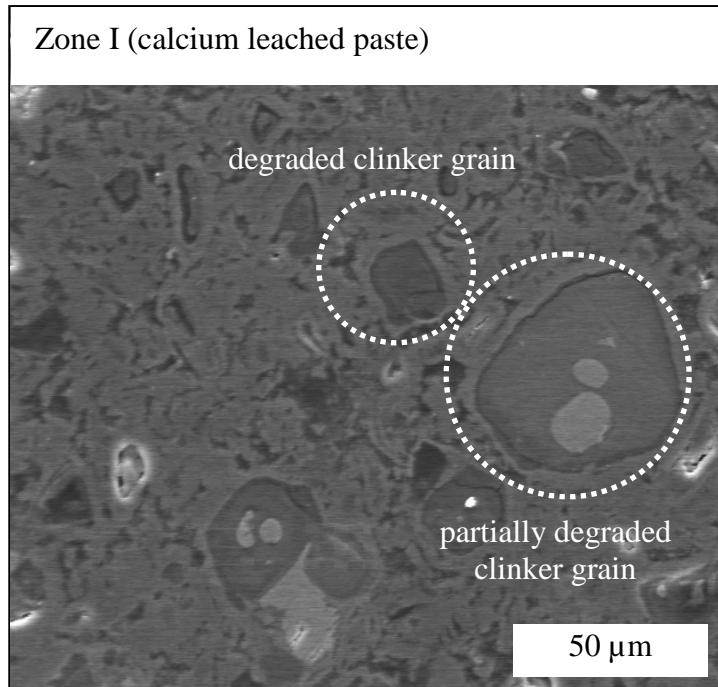


Fig. 7 porous texture of the degraded cement paste, dark colour of formerly unhydrated clinker grains indicates the decrease in density.

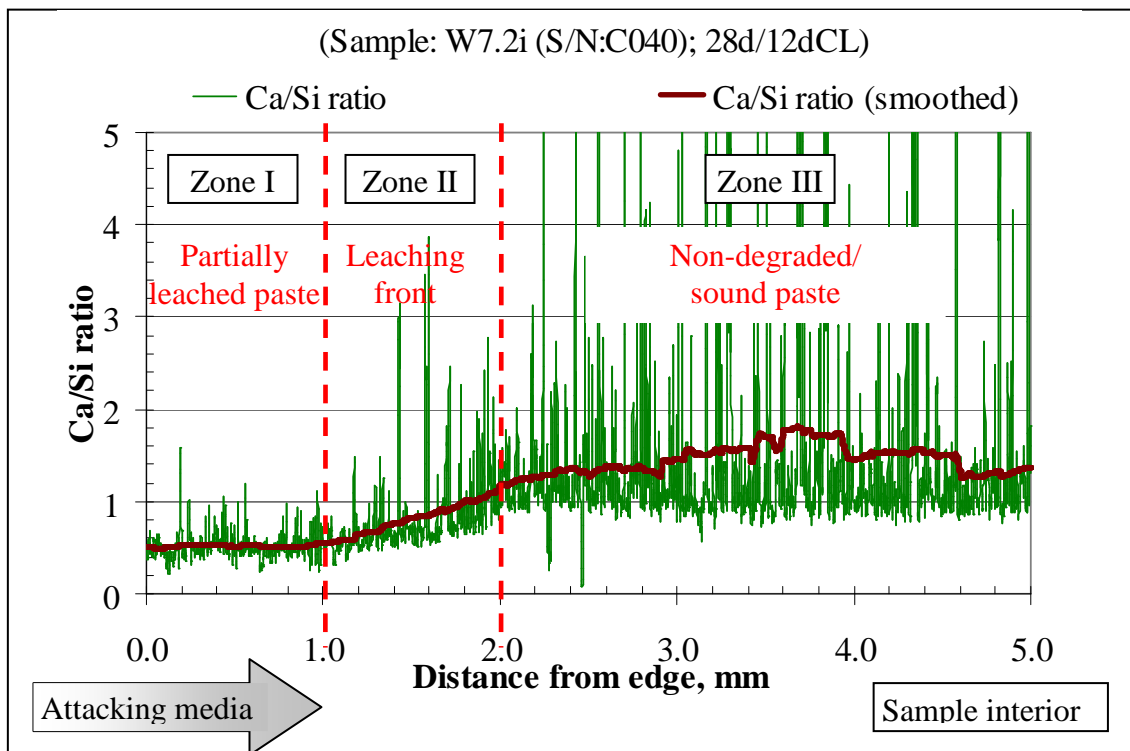


Fig. 8 Ca/Si ratio on partially leached WOPC.

Comparison of SEM imaging with Ca/Si ratio in WOPC paste

The mechanical performance of cementitious materials is supposed to be linked to the Ca/Si ratio of the hydration products [2, 3]. C-S-H gel is the main hydration product of hardened Portland cement and mainly contributes to its strength. A change in structure and calcium content will not only impact the mechanical performance of this phase but also the hardened paste. The decrease in Ca/Si ratio is caused by the dissolution of calcium due to leaching while the silica content remains. Fig. 5, Fig. 6 and Fig. 7 present images of three areas within a partially leached WOPC sample; an area of sound unleached paste (a), an area of incipient leaching (the leaching front b) and the fully leached zone (c). Fig. 8 presents details of an EDS line-scan traverse across the same sample, from the exterior (fully leached) to interior (unleached sound paste). Figures 5 - 7 are SEM secondary electron images of the paste microstructure, so exhibit mainly topographical information. However, it is clear from the images that there is a phase contrast evident, in the grey values of the different phases present, making them similar in appearance to a BSE image. Notwithstanding the contribution of phase composition and density to the grey intensity of a SE image, we interpret the appearance of the phases to be due in part to the overall low surface roughness of the samples allowing the specific roughness of each phase (dependant on its hardness, density and porosity) to affect the electron response.

The material beyond the 'leaching front' in the sample interior appears in the SEM image (Fig. 4) as sound, unaffected by the attacking 6M ammonium nitrate solution. It displays a typical relatively heterogeneous structure consisting of hydration products (CH, C-S-H) and unhydrated clinker grains. This is supported by the results of the EDS analysis of this area (line scan in Fig. 8) which show an average Ca/Si ratio of roughly 1.7, typical for hydrated Portland cement paste [14]. The various large spikes in the Ca/Si diagram can be interpreted as phases rich in calcium but low on silica such as C_2S , C_3S , and the largest as CH and gypsum.

Within the roughly 1 mm wide 'leaching front' (1 mm away from the outer edge of the specimen) the Ca/Si ratio decreases with proximity to the sample edge and from a level above 1 (see Fig. 8 from right to left). The decrease in Ca/Si scattering and in averaged Ca/Si concentration suggests the existence of more degraded hydration products and clinker particles. The SEM image of this area (Fig. 6) confirms the observations obtained from the EDS analysis. A change in colour (from white to grey) in the transition zone of the clinker grains indicates their beginning degradation (Fig. 6), highlighting narrow coronas of alteration around the grains. Due to the progression of calcium dissolution the appearance of C-S-H gel changes from more heterogeneous towards the sample centre to more homogeneous in the leached zone. However, the relatively smooth line of Ca/Si ratio towards the sample exterior within the 'Leaching front' implies that CH (which is most severely affected by calcium leaching) has been dissolved completely (Fig. 8).

The calcium leached cement paste appears, compared with the unleached material, as a relatively homogeneous (but porous) material (Fig. 7). This is in very good agreement with results obtained from EDS analysis. A low Ca/Si ratio of the leached paste within the exterior 1mm of the sample can be clearly seen (Fig. 8). An average Ca/Si ratio of approximately 0.5 and the absence of larger Ca/Si ratio peaks (over 1.5) indicate that hydration products and unhydrated clinker grains have been leached to a consistently low calcium level, hence the more homogeneous appearance in the SEM image (Fig. 7). The dark appearance of areas originally occupied by the un-hydrated clinker grains suggests an even less dense texture than those for degraded C-S-H phases.

Ca/Si ratio and mechanical performance in OPC and WOPC paste

The mechanical performance of the hydrated and unhydrated particles in the both OPC and WOPC paste was also studied using nanoindentation. In order to observe the gradual change in mechanical performance, at first 400 indents arranged in 4 rows of 100 indents each with 50 μm spacing, were made in the same area that was also studied by SEM/EDS, following a traverse from the exterior to interior of the samples. For the analysis of the experimental data only results within the range for hydration products (0 to 45 GPa) were considered.

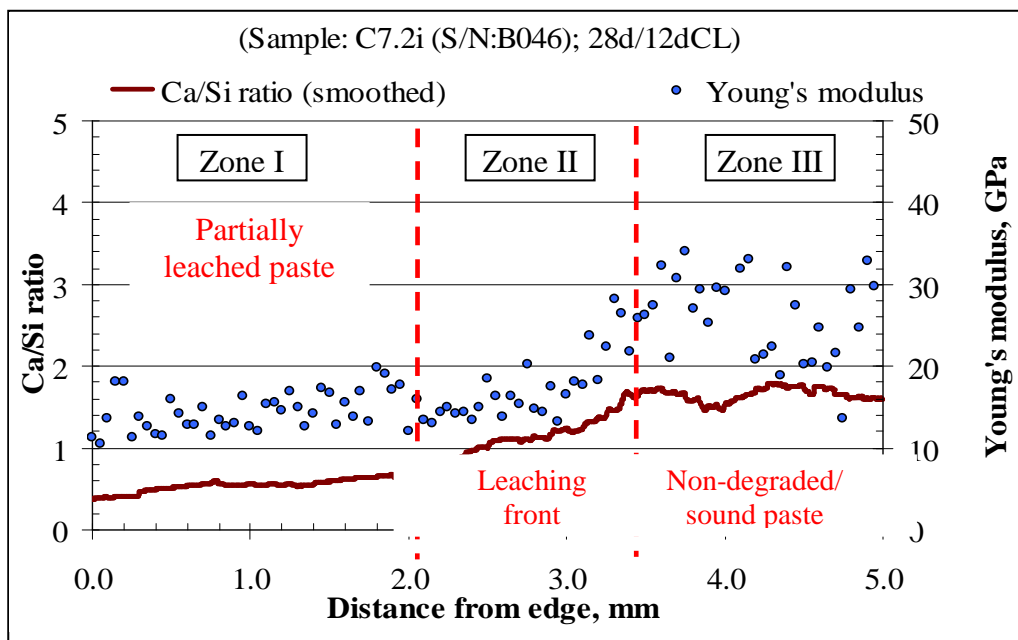


Fig. 9 Ca/Si ratio vs. Young's modulus on partially leached OPC.

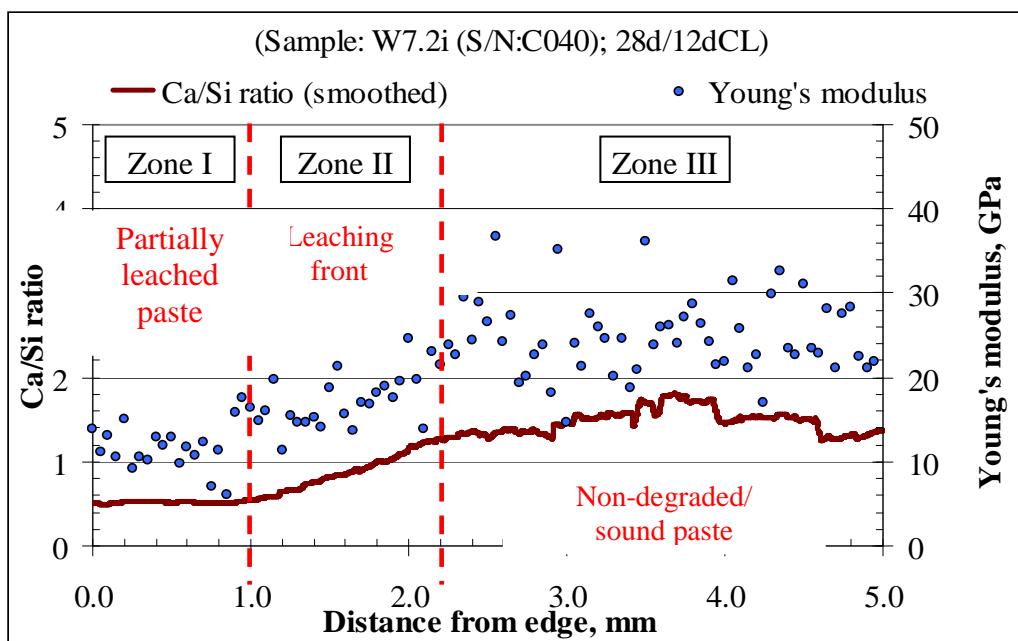


Fig. 10 Ca/Si ratio vs. Young's modulus on partially leached WOPC.

A strong link between Ca/Si ratio and Young's modulus values can be seen clearly in the *Ca/Si ratio vs. Young's modulus* diagrams for OPC (Fig. 9) and WOPC (Fig. 10). The rate of reduction in mechanical performance with leaching is similar to the decreasing calcium content due to calcium leaching. Comparing the Ca/Si in the external 2 mm, the results appear to suggest a better leaching performance for WOPC as the leaching front is only 1 mm away from the exterior of sample, and for OPC it is at 2 mm from the surface. The Table 2 below presents a summary of the results obtained from partially leached cement paste specimens. In spite differences in the leaching progress, both pastes show similar mechanical performances at the different stages of hydration.

Table 2 Ca/Si ratio and Young's modulus of degraded and non-degraded cement pastes

	OPC		WOPC	
	Ca/Si	<i>E</i> modulus	Ca/Si	<i>E</i> modulus
Degraded paste (Zone I)	0.54	14.6 GPa	0.51	11.7 GPa
Leaching front (Zone II)	0.96	15.0 GPa	0.80	16.5 GPa
Non-degraded paste (Zone III)	1.61	25.4 GPa	1.46	24.6 GPa

DISCUSSION

The most obvious structural change caused by calcium leaching can be observed with SEM microscopy. With the loss of calcium a transformation takes place converting a formerly heterogeneous paste into a porous material of almost homogeneous appearance. However, such analysis only allows rough estimates on the degradation progress of cementitious materials. It has been widely agreed that the strength of hardened ordinary Portland cement paste stands in close relationship to the calcium content of its hydration products. Thus, we have carried out additional tests engaging EDS analysis and nanoindentation testing on specimens only leached in the outer region of the sample. A number of indentations were performed following a traverse from the exterior to the interior of the samples, later to be studied by EDS. The results obtained from nanoindentation provide an average measure of the micromechanical performance of the tested area, which is compared with the Ca/Si ratio obtained from EDS within the line of indents. For both, OPC and WOPC paste the created diagrams show a good correlation between change in Ca/Si ratio and Young's modulus. This confirmed, as expected, the strong relationship of calcium content and strength of cementitious materials. The limitations of our test setup (50 μm indent spacing and the limited number of results) do not allow a reliable statistical analysis to determine phase specific properties) at this stage we obtained only the compound response of the tested paste. The experiments carried out on partially calcium leached specimens only represent the initial stage leaching showing still a considerably high Ca/Si of roughly 0.5 in both degraded pastes. But for OPC the leaching progress went 1 mm further than for WOPC which appears to suggest a better leaching performance for WOPC at this stage of degradation.

CONCLUSIONS

The sample preparation of highly heterogeneous materials consisting of phases with a large contrast in mechanical properties requires a lot of effort to achieve the surface quality required

for performing reliable nanoindentation experiments. Much care was needed to support the weak structure of calcium leached paste during the polishing process without interfering with the remaining properties of the different phases. The sample preparation procedure that was developed, of low stiffness resin impregnation with a gentle 'long-term - low speed - low contact pressure' not only allowed the production of sample surfaces of low flatness, but also without the loss of weaker phases in the process.

The loss of calcium due to calcium leaching causes changes in the micro-structure of cementitious materials easily observable by scanning electron microscopy. The transformation from calcium-rich highly heterogeneous paste into a very porous homogeneous material low in calcium is not the only consequence of calcium leaching. More important is the significantly decreased mechanical performance observed in the nanoindentation experiments. EDS analysis together with nanoindentation experiments were carried out within the same area on each specimen. The results from both techniques correlate very well and confirm/support the theory of a very close relation between Ca/Si ratio and the mechanical strength of hardened cement paste. It could be concluded that the mechanical performance reduces at a similar rate as the calcium content dissolves with the progress of calcium leaching.

ACKNOWLEDGEMENTS

Firstly, the authors gratefully acknowledge the financial support of the CODICE project by the European Commission under project FP7-NMP3-SL-2008-214030. Furthermore, we would like to express greatest thanks for help and support to all the other partners within the research project: Eduardo Torroja Institute for Construction Science (IETcc) (Spain), FUNDACION LABEIN (Spain), Technische Universiteit Delft (The Netherlands), Rheinische Friederich-Wilhelm-Universität Bonn (Germany), CTG S.p.A. (Italy), Morteros y Revocos BIKAIN, S.A. (Spain) and BASF SE (Germany). Liz Porteous at UWS is thanked for her ever excellent and essential assistance in operating the FESEM.

REFERENCES

- 1 Faucon, P., Le Bescop, P., Adenot, F., Bonville, P., Jacquinet, J.F., Pineau, F. and Felix, B., Leaching of cement: study of the surface layer, *Cement and Concrete Research* 26 (1996) 1707-1715.
- 2 Carde, C. and Francois, R., Leaching of both calcium hydroxide and C-S-H from cement paste: modeling the mechanical behavior, *Cement and Concrete Research* 28 (1996) 1257-1268.
- 3 Carde, C. and Francois, R., Effect of the leaching of calcium hydroxide from cement paste on mechanical and physical properties, *Cement and Concrete Research* 27 (1997) 539-550.
- 4 Carde, C. and Francois, R., Modelling the loss of strength and porosity increase due to the leaching of cement paste, *Cement and Concrete Composites* 21 (4) (1998) 181-188.
- 5 Gerard, B., Le Bellego, C. and Bernard, O., Simplified modelling of calcium leaching of concrete in various environments, *Materials and Structures* 35 (2002) 632-640.
- 6 Thomas, J.J., Jeffrey, J., Allen, A.J. and Jennings, H.M., Effects of decalcification on the microstructure and surface area of cement and tricalcium silicate pastes, *Cement and Concrete Research* 34 (2004) 2297-2307.

- 7 Kazuko, H. and Masahito, S., Change in pore structure and composition of hardened cement paste during the process of dissolution, *Cement and Concrete Research* 35 (2005) 943-950.
- 8 Gaitero, J.J., Campillo, I. and Guerrero, A., Reduction of the calcium leaching rate of cement paste by addition of silica nanoparticles, *Cement and Concrete Research* 38 (9) (2008) 1112-1118.
- 9 Oliver, W.C. and Pharr G.M., An improved technique for determining hardness and elastic modulus using load and displacement sensing indentation experiments. *Journal of Materials Research* 7 (1992) 1564-1583.
- 10 Oliver, W.C. and Pharr G.M., Measurement of hardness and elastic modulus by instrumented indentation: Advances in understanding and refinements to methodology. *Journal of Materials Research* 19 (2004) 3-20.
- 11 Constantinides, G., Ulm, F.-J. and Van Vliet, K., On the use of nanoindentation for cementitious materials. *Materials and Structures* 36 (2003) 191-196.
- 12 Ulm F., Vandamme M., Bobko C., Ortega J,A., Tai, K. and Ortiz, C., Statistical indentation techniques for hydrated nanocomposites: concrete, bones and shale. *Journal of the American Ceramic Society* 90(9) (2007) 2677-2692.
- 13 Sorelli, L., Constantinides, G., Ulm, F.-J. and Toutlemonde, F.,. The nano-mechanical signature of Ultra High Performance Concrete by statistical nanoindentation techniques, *Cement and Concrete Research* 38 (2008) 1447-1456.
- 14 Richardson, I.G.: The nature of C-S-H in hardened cements, *Cement and Concrete Research* 29 (1999) 1131–1147.